Research Square

Preprints are preliminary reports that have not undergone peer review.
They should not be considered conclusive, used to inform clinical practice,
or referenced by the media as validated information.

Coaxial cell printing of a human glomerular model *in vitro* of the glomerular filtration barrier and its pathophysiology

Narendra Singh
Pohang University of Science and Technology
Jae Yun Kim
Pohang University of Science and Technology
Jae Yeon Lee
Daegu Haany University
Hyungseok Lee
Kangwon National University https://orcid.org/0000-0003-0630-5772
Ge Gao
Beijing Institute of Technology
Jinah Jang
Pohang University of Science and Technology
Yong Kyun Kim
The Catholic University of Korea
Dong-Woo Cho (dwcho@postech.ac.kr)
Pohang University of Science and Technology https://orcid.org/0000-0001-5869-4330

Article

Keywords:

Posted Date: February 21st, 2022

DOI: https://doi.org/10.21203/rs.3.rs-1346352/v1

License: This work is licensed under a Creative Commons Attribution 4.0 International License.
Read Full License

Abstract

Many efforts have been expended in the emulations of the kidney's glomerular unit because of its limitless potential in the field of drug screening industry and nephrotoxicity testing in the clinics. Herein, we have fabricated a functional bilayer glomerular microvessel-on-a-chip that recapitulates the specific arrangement of glomerular endothelial cell (GE), podocyte layers, and the intervening glomerular basement membrane (GBM) in a single step. Our perfusable chip allows for the coculture of the monolayer glomerular endothelium and podocyte epithelium that display mature functional markers of glomerular cells, and their proper interactions produce GBM proteins, which are the major components of the GBM in vivo. Furthermore, we tested the selective permeability capacity, a representative hallmark function of the glomerular filtration barrier. Lastly, we evaluated the response of our glomerular model to Adriamycin- and hyperglycemia-induced injury to evaluate its applicability for drug screening and glomerular disease modeling.

Introduction

The glomerulus—a highly intricate and specialized glomerular capillary tuft that is enclosed in the Bowman's capsule—is the most vital functional constituent of the systemic kidney [1, 2]. The essential function of the glomerular capillaries is to filter the circulating blood such that the important plasma proteins (e.g., macromolecules) are retained in blood, and small to middle-sized solutes in the plasma are excreted as urine. The function of the glomerular filtration barrier (GFB) is dependent on the meticulous arrangement and cellular crosstalk among its three main components: the glomerular endothelial cells (GEs), the intervening glomerular basement membrane (GBM), and the highly specialized podocytes, an epithelial cell type (with a footprint-like structure) [3, 4]. Damage to these GFB constituents leads to severe glomerular dysfunction associated with the loss of selective ultrafiltration capability [5-7]. Approximately 10% of the population worldwide has suffers from chronic renal disease which subsequently progresses to end-stage renal disease (ERSD) [8].

Unfortunately, new therapeutic approaches for chronic renal disease or precise screening of drug-induced nephrotoxicity models are held back by the lack of appropriate *in vitro* functionalities of the GFB, which includes complex cell-matrix interaction and cellular crosstalk among its constituents. Hence, the development of an *in vitro*, human kidney glomerular model that can mimic the *in vivo* phenotype and function would greatly advance the field of drug discovery and illuminate the mechanism of glomerular pathophysiology.

In this context, few *in vitro* models have been developed to mimic the functional unit of GFB [9-12]. For example, Musah et al. demonstrated a polydimethylsiloane (PDMS)-based microfluidic platform that encompassed two microfluidic channels parted by an extracellular-matrix-coated-PDMS porous membrane, in which the GEs and podocytes were respectively seeded on the top and bottom sides of the porous membrane [10]. However, this *in vitro* model relies on complicated processes with multiple steps making the fabrication process more error-prone. Furthermore, the synthetic porous PDMS membrane

that separates the podocytes and GEs lacks a selective filtration barrier, and leads to an unrestricted flow of media and molecules through its pores. In addition, the deviation of the membrane's thickness from that in the native GBM state prevents the proper crosstalk between GEs and podocytes. This constitutes the key limitation of synthetic glomerular emulations.

Another notable approach involves the kidney organoids—derived from pluripotent stem cells that offer the generation of immature nephron-like structures—that reiterate some characteristics of the glomerular microenvironment [13-15]. While this approach is remarkable, it has limited glomerular filtration activity owing to the failure to replicate the functional vascular circuit and the formation of GBM. Most importantly, the kidney organoids generated from the pluripotent stem cells requires complicated nephrogenic induction procedures that may limit the capacity to control tissue morphology and function [14, 15].

Recently, glomerulus-on-a-chip was developed with the use of a three-lane organoplate [11]. The podocytes and GEs were seeded on collagen-coated perfusion channels and demonstrated glomerular filtration function. Although this chip does contain cellular and protein GBM components, the bidirectional fluid flow condition proposes a critical limitation in reflecting the one-sided flow of the native glomerulus. Thus, we hypothesized that the discrepancy from the native flow state caused by the bidirectional flow in this chip is unsuitable for recapitulating the native function of GFB [16, 17]. Therefore, the advent of a clinically relevant GFB remains challenging. This necessity inspired the development of a glomerular equivalent, *in vitro* GFB model that mimics precisely the native structure and function of GFB and its pathophysiology in response to various stimuli.

Other recent studies showed that the three-dimensional (3D) coaxial cell printing technique has gained remarkable attention in the effort to print the perfusable tubular structures by the co-printing of multiple biomaterials based on numerous concentric channels [18-21]. As far as it is known, no attempts have been expended so far for the printing of a glomerular model for recapitulating correct glomerular filtration function, and for studying mechanisms of glomerular pathophysiology *in vitro*.

In this study, a functional bilayer glomerular microvessel-on-a-chip (bGOAC) that encompasses the inner monolayer of GEs and outer layer of podocytes was fabricated for the first time in a single, continuous process, using a coaxial cell-printing technique and an optimized tissue-specific hybrid kidney bioink (Fig. 1, A-C). Our perfusable bGOAC caused the rapid formation and geometrical assembly of glomerular endothelium and the podocyte epithelium mimicked the native glomerulus. Most importantly, correct interaction and crosstalk between the GEs and podocytes generated abundant *de novo* human collagen type IV (COL IV) and laminin (LAM), which are the major proteins of the GBM. Our glomerular model recapitulates the selective permeability function of GFB and response to drug-induced GFB dysfunction and proteinuria *in vitro.* Finally, we showed that the bGOAC model provides distinctive features suitable for exploring renal pathophysiological studies, such as diabetic nephropathy, by inducing high-glucose conditions. These findings suggest that the developed bGOAC could provide a novel platform for the

study of glomerular function, drug-induced nephrotoxicity, and mechanisms of glomerular pathophysiology *in vitro*.

Results

Functional assessment of glomerular cells with hybrid bioink for coaxial cell printing

Tissue decellularized extracellular-matrix-based bioinks have been extensively applied in tissue engineering and 3D cell printing of tissues/organs to provide the tissue-specific native microenvironment to the resident cells [22-24]. Recently, studies have reported the use of alginate blended with decellularized tissue bioinks to achieve the mechanical properties suitable for 3D coaxial cell printing [18, 21]. To obtain printable bioinks for 3D coaxial cell printing of functional bGOAC, we first customized the hybrid bioink formulation by blending sodium alginate with KdECM bioink to promote cellular activity of GEs and podocytes.

We first assessed the cell viability and gene expressions of podocytes and GEs encapsulated independently in hybrid bioinks at different proportions of KdECM and sodium alginate (Supplementary Fig. 1A, B). After 7 days of culture, we observed significant increments in cell viability and gene expressions in glomerular cells (podocytes and GEs) encapsulated in the hybrid bioink at an equal ratio of 3% (w/v) KdECM mixed with 1% (w/v) sodium alginate (i.e., 3K1A). The values were superior to 3% (w/v) KdECM mixed with 2% (w/v) sodium alginate (i.e., 3K2A) and 3% (w/v) of pure sodium alginate (Supplementary Fig. 1A, B). Upon confirmation of the 3K1A bioink as our optimized hybrid bioink ratio, we compared the biological performance of the 3K1A with 3% (w/v) pure KdECM and 3% (w/v) collagen type I, an extensively used bioink for kidney tissue engineering. The customized hybrid bioink (3K1A) displayed superior cell viability for the GEs and podocytes compared with collagen type I (Fig. 1D, E, and Supplementary Fig. 2). Moreover, we also observed higher expressions of the vascular maturation marker for endothelial junctions (CD31) and podocyte-specific markers (podocin and nephrin) based on immunofluorescence staining of GEs and podocytes encapsulated in independent groups. The overall expressions of the cells encapsulated in hybrid bioink (3K1A) was higher than those in collagen type I bioink, but lower than those in pure KdECM bioink (Fig. 1F-H).

The customized hybrid bioink (3K1A) maintained high-cell viability, upregulated expression levels of vascular markers of glomerular endothelial cells, and podocyte markers.

Subsequently, we printed GEs and podocyte-laden bioinks using coaxial cell printing. This resulted in the formation of monolayered, hollow GE and podocyte tubes that are capable of perfusion in standard cell culture conditions (Fig. 2A, B). Both monolayered hollow tubes (GE and podocyte) exhibited a homogeneous distribution of cells in their respective tube walls. The live/dead images of the encapsulated cells in their respective monolayered hollow tubes showed prominent cell viability without distortions in tube structural fidelity after 7 days of culture (Fig. 2A, B).

We also confirmed based on immunofluorescence staining the sustained expressions of CD31 and zonula occludens (ZO-1) markers in the GE tube, and nephrin and podocin in the podocyte tube (Fig. 2C-H). These findings suggest that the markers CD31, ZO-1 in the GE tube, and nephrin and podocin in the podocyte tube were articulated along with their maturation process. The overall results of coaxial cell printed GE and podocyte hollow tubes indicate a promising applicability potential for glomerular printing.

Therefore, the 3K1A hybrid bioink was utilized to carry both GEs and podocytes for the printing of functional GFB.

In vitro modeling of glomerular filtration barrier

To date, several *in vitro* proximal tubule models have been introduced by microfluidics or 3D cell printing techniques [21, 25-27]. In contrast, 3D cell printing of functional glomerular structure, has not yet been reported, and remains an ambitious goal. Using a coaxial cell printing method, we intended to replicate the specific glomerular barrier structure (inner layer: GEs, outer layer: podocytes and intervening GBM) by fabricating a bGOAC and evaluating whether this *in vitro* glomerular model could be utilized to examine the function of GFB, screen nephrotoxic drugs, and be used as the study of glomerular pathophysiology.

The functional bGOAC was prototyped using the customized bioink and coaxial cell printing process (Fig. 3 and Supplementary Movie 1). The fabrication process of the bGOAC involves the printing of a poly(ethylene/vinyl acetate) (PEVA)-based bGOAC chip body, coaxial cell printing of bilayer glomerular microvessel, and the fixation of the inlet–outlet of the printed bGOAC using agarose (Fig. 3A, i-iii, and 3B, i-iii). To visualize the discriminated inner layer (representing the monolayer of GEs) and outer layer (representing the monolayer of podocytes) of the glomerular model, we labeled inner and outer layers of the bilayer glomerular microvessel using red and green fluorescent beads, respectively. Both inner and outer layers of the printed, hollow, bilayer glomerular microvessel were successfully envisioned in its predefined place (Fig. 3C, D).

Figs. 3E and 3F represent the cross-sectional view of the printed, hollow, bilayer glomerular microvessel, reflecting distinctly defined inner and outer layers, each colored in either green or red. Despite the discriminated bilayers, the wall thickness of the inner and outer layers that respectively load GEs and podocytes, should be minimized to assist the formation of monolayer GEs and a podocyte layer. On average, the inner and outer diameters of the hollow bilayer glomerular microvessel were measured to be equal to 542 ± 41 and 684 ± 57 μm, respectively, whereas the inner and outer wall thicknesses (WTs) of the hollow bilayer glomerular microvessel were 71 ± 10 and 122 ± 24 μm, respectively (Fig. 3G, H).

Moreover, the inner/outer dimensions and layer thicknesses of the printed hollow bilayer glomerular microvessel were easily tuned [18, 20, 21]. A perfusion test was performed with the optimized bGOAC (Fig. 3B, iv, and Supplementary Movie 2). During the entire perfusion process, the printed, bilayer glomerular microvessel lumen maintained good structural integrity without any leakage.

Upon the establishment of fabrication parameters, we cell printed the bGOAC using GEs and podocytes encapsulated individually in the customized hybrid bioinks (Fig. 4). The coaxial cell-printed, hollow glomerular microvessel possessed two distinct layers, with the inner layer containing the GEs, and the outer layer containing the podocytes. To allow cultures in the fabricated bGOAC, a peristaltic pump was connected to allow the circulation of GEs and culture media through the bilayer glomerular microvessel. This provided media to the GEs of the inner layer, while the podocyte culture media was supplied through the urinary compartment to support cellular growth in the outer layer of the bilayer glomerular microvessel. The viability of both cells in the wall of the printed bilayer glomerular microvessel was maintained on day 1 (~95%) and remained high until day 7 (~97%) (Fig. 4A, i, ii). Likewise, in a separate experiment, the bGOAC was stained for CD31 and nephrin on days 3 and 7 to observe the cellular phenotype within the printed bilayer glomerular microvessel (Fig. 4B-F). The mature and confluence expressions of CD31 and nephrin necessary for proper function of GFB was detected in the fabricated bGOAC, thus suggesting that the encapsulated GEs in the inner layer and podocytes in the outer layer of the bilayer glomerular microvessel generated the intact endothelium and epithelium, respectively (Fig. 4B-F). More importantly, mature expression of the critical tight junction marker ZO-1 was also verified on day 7 (Fig. 4G). To evaluate the long-term preservation of the cellular phenotype in the printed glomerular model, the marker expressions of CD31, tight junction ZO-1, and nephrin, were validated after 14 days. This confirmed the stable expressions and maintenance of these markers in the bGOAC (Supplementary Fig. 3A, B).

These results confirmed the successful fabrication of *in vitro* GFB on a chip via the coaxial cell printing method and our customized bioinks.

The recreation of correct functional GFB is a critical requirement for the development of a new therapeutic approach to chronic kidney disease as well as for the study of glomerular pathophysiology. Podocyte and GE layers in the developed GFB may not fully assure the correct function of glomerular capillary wall without the existence of GBM. During kidney development, podocytes and GEs are accountable for the synthesis of the GBM composition in the glomerular capillary wall [28, 29]. In human GBM, COL IV, and LAM are its major structural components necessary for its function, as mutations in COL IV and LAM cause filtration defects and result in human kidney disease [30, 31].

We confirmed the deposition of COL IV and LAM in the printed podocyte tube, monolayer GE tube, and bGOAC on day 7. The immunofluorescence staining results verified the significant production and deposition of the COL IV and LAM proteins in the printed bGOAC, monolayer podocyte, and GE tubes (Fig. 5A, B). In addition, these results also revealed that production of COL IV and LAM were predominantly high in the podocyte tube compared with the GE tube, thus confirming that podocytes were mainly accountable for the assembly of these GBM proteins. *In vivo* GBM formation was directly associated with the interactions of the podocyte–GE cells. Thus, synthesis of neo-GBM in the bGOAC revealed the correct interaction and cellular crosstalk between the podocytes and GEs. This demonstrated that the coaxial, cell-printed bGOAC resembles the *in vivo* GFB.

Permselectivity function of the printed bGOAC

One important function of the GFB is to filter the molecules in the bloodstream based on their sizes [2]. *In vivo*, the GFB is a highly specialized interface that retains large solutes (i.e., albumin) within the plasma while allowing higher conductance toward small to midsized solutes (i.e., inulin. Under the physiological condition, albumin is retained within the blood, whereas albumin leakage in the urine reflects the dysfunction of the GFB [10]. We then conducted tests to assess whether printed bGOAC could also reconstitute the permselectivity function. For this, we perfused large molecules such as fluorescein isothiocyanate (FITC)–albumin and FITC–dextran (70 kDa) into the lumens of mature bGOAC, and in the monolayer GE, podocyte, and bare tubes (without cells).

The perfusable bGOAC prevented the large molecules (albumin and dextran) from leaking (Fig. 5 C and D) at 3 min, 20 min, and 30 min. More than 99% of albumin was retained within the bilayer glomerular microvessel after perfusion for 1 h (Supplementary Fig. S4). We also analyzed the albumin permeability within monolayer GE and podocyte tubes. Both monolayer GE and podocyte tubes exhibited moderately selective permeability toward albumin compared with bilayer glomerular microvessel (Supplementary Fig. S4). In addition, the podocyte tube retained albumin to selectively higher levels compared with the GE tube levels, thus demonstrating the podocytes to be the key player of albumin selective permeability in the bGOAC. To show the superiority of our glomerular model to other *in vitro* models, we have compared our bGOAC with the transwell, cocultured podocyte–glomerular endothelial barriers. The supplementary Fig. S4 revealed that the transwell coculture GFB displayed a pronounced leakage of albumin as compared with our cell-printed bGOAC, hence, indicating that the transwell, coculture podocyte–endothelial barrier is unable to execute as efficiently as the cell-printed bGOAC.

Furthermore, we evaluated the filtration capability of our fabricated bGOAC for inulin a small-sized molecule, as it is performed by *in vivo* GFB. Fig. 5E shows that inulin can freely pass the GFB-containing bilayer glomerular microvessel to the urinary compartment of bGOAC. These findings suggest that the cell printed bGOAC specifically replicates the normal function of the *in vivo* GFB that is able to perform the differential clearance of large and small molecules, as illustrated by the albumin and inulin outcomes.

In vitro modeling of drug-induced glomerular injury and proteinuria

In clinical therapeutics, drug-induced nephrotoxicity (DIN) is often inevitable and remains a major hurdle [32]. Hence, an accurate prediction tool for DIN is of critical relevance as it can avoid renal damage to patients who are undergoing drug-based therapy. Additionally, the possibility to customize the design of drug types and doses based on the utilization of a functional screening glomerular system *in vitro* is envisaged to have tremendous value for the prediction of DIN and/or for new drug development.

To test the hypothesis that our cell-printed functional bGOAC represents a distinctive model for screening drug-induced glomerular injury state, we exposed the cell-printed glomerular model to various doses of Adriamycin for 3 days via perfusion through the bilayer glomerular microvessel (Fig. 6A). The cell viability in the bilayer glomerular microvessel was evaluated after treatment with different concentrations of

Adriamycin (Fig. 6B, C). Cell viability in the bilayer glomerular microvessel was reduced after Adriamycin treatment. Notably, the podocyte functional genes (nephrin, podocin), endothelial cell-specific genes (CD31, eNOs), and tight junction marker (ZO-1) were also significantly decreased in the bilayer glomerular microvessel exposed to Adriamycin (Fig. 6D). In contrast, inflammatory marker VCAM-1 expression levels were drastically upregulated after Adriamycin exposure to the bilayer glomerular microvessel. Further, the immunofluorescence staining with ZO-1 and nephrin also confirmed the Adriamycin-induced injury state of the glomerular bilayer (Fig. 6E, F).

Proteinuria is routinely used in the clinic to assess renal injury (glomerular damage) [11]. We have also assessed the albumin barrier function of bGOAC with and without treatment by perfusing the large molecular complex FITC–albumin. The glomerular chip treated with Adriamycin displayed remarkable albumin loss from the bilayer glomerular lumen and augmented the level of albumin leakage into the urinary part (Fig. 6G), as is detected in the course of Adriamycin-induced glomerular damage *in vivo*. Furthermore, the quantitative albumin clearance from the bGOAC was evaluated by perfusing FITC–albumin to normal and Adriamycin-injured glomerular microvessels (Fig. 6H). The printed glomerular model exposed with Adriamycin displayed substantial albumin leakage from the bilayer glomerular microvessel (40% loss of albumin) and increased albumin entry into the urinary part (Fig. 6H).

Diabetic nephropathy modeling within bGOAC

Diabetic nephropathy is a severe diabetic microvascular complication due to inadequate glycemic control, and is responsible for progressive kidney disease in diabetic patients. Hyperglycemia-associated injury of renal glomerular endothelial cells is acknowledged as the main instigation factor of diabetic nephropathy pathogenesis in diabetic conditions. Consequently, albumin leakage across the GFB is increased, which is an important pathological characteristic of diabetic nephropathy.

To demonstrate that our cell-printed bGOAC could mimic the hyperglycemia-induced glomerular injury, we perfused the media containing various concentrations of glucose (5, 15, 20 mM) in mature bGOAC for 3 days (Fig. 7A). Interestingly, we observed that exposure to high glucose concentration upregulated the expression level of the inflammatory marker intercellular adhesion molecule 1 (ICAM-1), and downregulated the expression of the glomerular functional markers (nephrin, eNOs) (Fig. 7B).

In addition, immunostained bGOACs with nephrin and ZO-1 showed that the expressions of nephrin and ZO-1 were drastically suppressed in diabetic bGOAC compared with normal bGOAC (Fig. 7C, D). The suppression of the tight junction protein ZO-1 expression in the injured glomerular leads to the enlargement of the filtration barrier. As a result, albumin clearance is promoted, which is the key clinical sign of diabetic nephropathy (Fig. 7E-G).

Altogether, results demonstrate that this cell-printed glomerular model signifies a distinctive platform to study glomerular pathophysiology.

Discussion

The lack of specific *in vitro* models of GFB limits the understanding of intricate signaling among the glomerular cells in the GFB, potential applicability for *in vitro* drug screening/drug discovery, and the study of glomerular pathophysiology. Therefore, we constructed a coaxial cell-printing-based functional glomerular structure on a chip that mimics the specific arrangement of monolayer GEs, podocyte layers, and the GBM in a single step that, to our knowledge, has not yet been fabricated in earlier *in vitro* models. To fabricate correct functional GFB *in vitro*, one of the key requirements is the development of a suitable bioink that can promote the activity of podocytes and GEs as well as retain the printed bilayer glomerular structural fidelity.

First, we confirmed the potential of KdECM as a valuable natural bioink for supporting the cellular behavior of both GEs and podocytes due to the broad maintenance of the intricate natural kidney components. Thus, altering the KdECM to obtain printable bioinks could allow the successful fabrication of functional bGOAC using coaxial cell printing. By blending with sodium alginate, the established hybrid KdECM bioink (3K1A) enabled 3D coaxial cell printing of glomerular structure and also maintained the functional performance of KdECM to support the biological behaviors of both GE and podocyte.

Using the cell laden hybrid KdECM bioink (3K1A), the 3D coaxial cell printing method allowed the direct fabrication of hollow monolayer of the tubes which encapsulated either GEs, podocytes, or both, by manipulating the extrusion modes of the coaxial nozzle. The endothelial cell specific marker CD31, tight junction marker ZO-1 in the GE tube, and podocyte-specific markers nephrin and podocin in the podocyte tube were confirmed as cell–cell interaction markers. With these advances, a perfusable, bGOAC that contains both GE and podocyte layers was printed in a single continuous process for the first time by turning on/off the triple coaxial channels. The printed bGOAC was cultured in perfusion conditions, evaluated the long-term cell viability, and maintained the mature level of endothelial cell- and podocyte-specific markers.

Moreover, each of the printed GEs and podocytes in bGOAC rapidly generated the matured endothelium and epithelium within 3 days. Most importantly, subject to *in vitro* chip culture conditions, abundant *de novo* human COL IV and LAM proteins were also observed, thus indicating the construction of well-assembled GBM in the bilayer glomerular microvessel that is important for the formation of the functional GFB.

Henceforth, we have established a convenient and viable approach for direct construction of *in vivo*-like GFB facilitated by correct interactions and crosstalk between the GEs, podocytes, and production of GBM.

Importantly, we verified glomerular permselectivity function within the fabricated mature bGOAC by perfusing large molecular complexes (FITC–albumin, FITC–dextran) and small molecules (e.g., inulin) into the lumens of bilayer glomerular microvessels. The cell-printed bGOAC prevented the leakage of large molecules (albumin and dextran) but freely filtered inulin in a manner similar to *in vivo* GFB cases, thus emulating the human GFB. This effective GFB realized by our cell-printed glomerular model can be justified by the proper crosstalk between the inner GE and outer podocytes layers, and by the correct

formation of GBM. In addition, we analyzed the albumin permeability within the monolayer GE and podocyte tubes. Interestingly, the podocyte tube retained albumin within the tube at levels higher than those in the GE tube, thus validating the assertion that the podocytes probably constitute one of the main factors of albumin-selective permeability in the glomerular structure. To show the superiority of our *in vitro* model to transwell systems, we compared our cell-printed glomerular model to the transwells which contained cocultured podocyte GE barriers. The transwell coculture GFB displayed a pronounced leakage of albumin compared with our developed glomerular model, and further emphasized the strength of our cell-printed glomerular model.

Previously, microfluidic-based *in vitro* models were fabricated to explore glomerular ultrafiltration. Nevertheless, these microfluidic devices do not demonstrate correct human glomerular microphysiological characteristics owing to the presence of an artificial porous membrane as GBM, and bidirectional fluid flow, and could not be utilized for accurate prediction of drug-induced nephrotoxicity. Our cell-printed, *in vitro* glomerular model consisted of glomerular endothelium, epithelium, and intervening assembly of GBM with unidirectional fluid flow that allowed the selective filtration measurement across the glomerular barrier. The cell viability, gene expression analysis, and immunofluorescence experiments investigated the morphological/cellular phenotypic alterations induced by different chemical stimuli treatments. The cell-printed glomerular model recapitulated the functional state of the normal human glomerular barrier, thus showing the permselectivity of solutes that could be modulated using Adriamycin –a chemical drug well recognized to persuade proteinuria *in vivo*. Additionally, the analysis of cell viability, gene expression levels, and immunofluorescence distribution of nephrin and tight junction marker ZO-1 establishes a connection among the cellular phenotype and functional events owing to exposure with Adriamycin. We believe that our coaxial cell-printed glomerular model is appropriate for the quick and precise testing of therapeutics and for the assessment of new drug nephrotoxicity. This opinion is justified by the fact that quantitative reverse transcription polymerase chain reaction and immunofluorescence assays that show the variation in the level of gene expressions and distribution of protein markers are linked with functional data. This model could be also explored for the screening of pharmaceutical drugs that could recover the glomerular filtration function after GFB injury.

Of pivotal relevance for the study of glomerular diseases, the cell-printed glomerular model offers a unique opportunity for glomerular disease modeling. Hyperglycemia is a well known factor used to initiate the diabetic nephropathy in diabetic patients, and was realized within the bGOAC. We showed that exposure of high concentrations of glucose to bGOAC drastically enhanced the inflammatory marker ICAM-1 and reduced glomerular cell-functional markers that promoted albumin leakage across the GFB. In brief, these findings indicated that the 3D cell-printed glomerular model replicates the normal human GFB, and constitutes a vital platform to conduct drug screening and study the mechanisms of glomerular disease pathophysiology.

We acknowledge that our *in vitro* model does not contain mesangial cells. Therefore, future studies will emphasize the printing of a triple-layer-glomerular structure using our printing strategies, permitting

culture and cellular interaction among GEs, and podocyte as well as mesangial cells in perfusable conditions. In conclusion, 3D coaxial cell-printed glomerular-on-a-chip represents a unique *in vitro* model that recapitulates the human glomerular filtration barrier, and constitutes an ultimate tool for the study of glomerular pathophysiological events and for the screening of nephrotoxic drugs.

Online Methods

Customization of hybrid bioink for coaxial cell printing of glomerular model

The kidney decellularized extracellular matrix (KdECM) bioink was prepared by the decellularization of fresh porcine kidney according to the previously optimized protocol with minor modifications [21]. The kidney tissue supplied from the slaughterhouse was sliced into small sections (~0.5 mm). The sliced kidney tissue was washed several times for 2 h using distilled water. It was then treated with 1% Triton X-100 at 25 °C for 24 h to remove the cellular components. Subsequently, the acellular matrix was washed and treated with deoxyribonuclease at 37 °C for 12 h. After washing with phosphate buffer saline (PBS), KdECM was sterilized with 0.1% antibiotic (peracetic acid) for 1.5 h. Finally, KdECM was washed again several times with PBS.

The KdECM was freeze-dried for 48 h, and was then dissolved in acetic acid (0.5 M) which contained pepsin to yield 4% of KdECM pregel. To formulate the hybrid bioinks for cell printing, blending of 4% (w/v) of KdECM pregel, and 8% of sodium alginate pregel was achieved by stirring vigorously for 24 h to obtain the homogeneous hybrid bioink solution. The pH values of the hybrid bioinks were adjusted to 7.4 by using a 10 M NaOH solution, and the concentration of KdECM and sodium alginate in hybrid bioinks was finalized by the addition of PBS. The 3% KdECM and 1% sodium alginate ratio in the hybrid bioink (termed as 3K1A) was used in subsequent experiments.

Cell culture and cell viability assay

Primary human podocytes and GEs (Celprogen, Canada) were cultured and expanded at 37 °C in 5% CO_2 using their respective culture media per supplier's directions. For all experiments, human primary podocytes and GEs were used at passages 4 to 7.

The biocompatibility study of hybrid bioinks at different formulations was implemented with primary human podocytes and GEs. The podocytes and GEs were encapsulated in the KdECM bioink, hybrid bioink, and collagen type I (Dalim Tissen, Korea). To crosslink the sodium alginate component in the hybrid bioinks, 0.1 M $CaCl_2$ was used to treat the hybrid bioinks before incubated at 37 °C. The live/dead assay kit from Thermo–Fischer Scientific was used to investigate the live/dead cells in the samples. The images of live/dead cells in the samples were captured by laser confocal microscopy. In addition, by following the supplier's protocol, Cell Counting Kit-8 (CCK-8; Dojindo, Japan) was used to analyze the metabolic activity of living cells of podocytes and GEs after 7 days of culture. The CCK8 reagent added to the cultured samples and absorbance of the supernatant were quantified at 450 nm with the use of a microplate reader.

3D cell printing of glomerular-microvessel-on-a-chip

To fabricate the bGOAC, the 3D coaxial cell printing was applied using our previously established Integrated Composite Tissue/Organ Building System and a customized coaxial nozzle with different diameters (14G/17G/22G) from Ramé-Hart Instrument, USA. The GEs (density: 1×10^7 cells mL^{-1}) and podocytes (density: 2×10^7 cells mL^{-1}) were laden in hybrid kidney bioinks (3K1A) and subsequently connected to middle and shell nozzles, respectively. The fugitive 30% Pluronic F127 from Sigma–Aldrich was solubilized in a 100 mM calcium chloride solution, and the final solution was termed as CPF127, which was further charged to core nozzle at 37 °C.

During the printing of the glomerular model, the chip body was fabricated by the extrusion of PEVA from Polysciences, USA. Subsequently, the bilayered glomerular tubule was fabricated by direct coaxial printing in the chip body using self-assisted coded programs. The thermosensitive low-melting agarose (LMA) from Thermo–Fisher Scientific, USA, was mounted in both the inlet and outlet of the glomerular chip. After gelation of the fabricated bilayer glomerulus microvessel tube, the fugitive CPF127 core materials were removed and finally bGOAC was connected to a peristaltic pump (LONGER, China) to perfuse the GE media at the flow rate in the range of 0.1–10 μL min^{-1} based on the bilayer glomerular microvessel diameter to mimic *in vivo* shear stress conditions until maturation. Meanwhile, podocyte media were supplied to the urinary part of the chip to culture the outer layer of podocyte in the bilayer glomerular microvessel.

Quantitative reverse-transcription polymerase chain reaction (RT-PCR)

Total ribonucleic acid was isolated following the supplier's protocol and materials of RNeasy Mini kit from the Qiagen, Germany, and its concentration was analyzed by Nanodrop spectrophotometer from Thermo–Fischer Scientific, USA. The complementary deoxyribonucleic acid (cDNA) synthesis kit from the Thermo–Fischer Scientific, USA was used to synthesize the cDNA, and the gene expressions levels were determined using SYBR-green from Thermo–Fisher Scientific, USA, through StepOne Plus RT-PCR system from Applied Biosystems, USA.

Primers and probes were designed as reported data of gene sequence references of the National Center for Biotechnology Information. The designed primers were purchased from Bioneer (Korea) (Table S1).

Immunostaining and confocal imaging

The harvested samples were washed with PBS and fixed thereafter using 4% buffered formalin for 1 h. The fixed samples were washed with PBS to remove the fixative, and subsequently permeabilization was performed with 0.1% Triton X-100 (Sigma, USA) in DBS for 10 min at room temperature. Subsequently, the treated samples were incubated with the blocking solution 3% bovine serum albumin at room temperature for 60 min. Subsequently, the primary antibodies podocin, nephrin, CD31, collagen IV (COL IV) from Abcam, USA, and ZO-1 (Bioss, USA), laminin (LAM) (Invitrogen, USA), diluted in 1% blocking bovine serum albumin were applied based on the manufacture's recommendation and incubated for 12 h

at 4 °C. The unbound primary antibodies from the treated samples were removed after washing several times with PBS. Secondary antibodies from Thermo–Fisher Scientific, USA, in 1% blocking solution bovine serum albumin were used to treat the samples for 2 h at room temperature. Furthermore, treated samples were washed with PBS and counterstained the nuclei with 4',6'-diamidino-2-phenylindole (DAPI) from Thermo–Fisher Scientific, USA. The stained samples were imaged with a confocal laser microscopy (Leica TCS SP5 II, Germany).

Inulin and albumin filtration assays

For the filtration studies, the media for GEs which contained FITC–inulin (10 μg/mL) or FITC–albumin (150 μg/mL) were perfused through the mature bGOAC for 1 h. The diffusion of FITC–albumin or FITC–inulin from the bilayer glomerular microvessel to the urinary compartment was captured by Nikon Eclipse Ti fluorescence microscope at 3 min, 20 min, and 30 min. The diffusional permeability was evaluated using the previously reported equation [18]. The leaked FITC–albumin in media were collected from the urinary compartment at 60 min, and the relative fluorescent intensities at the excitation (495 nm)/emission (520 nm) wavelengths were analyzed with a microplate reader (Hidex Sense 425-301) in 384-well polystyrene microplates.

Drug-induced injury

First, the printed bGOAC was cultured at 37 °C and 5% CO_2 for 7 days. Subsequently, Adriamycin, a nephrotoxic drug (LC Laboratories) was perfused in culture media through the matured bGOAC for 3 days to induce drug-mediated glomerular injury. The culture media were only perfused to the chip, and termed as "normal."

Hyperglycemia induced injury

To demonstrate the hyperglycemia induced glomerular injury in the fabricated glomerular model, GEs media with different concentrations of glucose (5 mM, 15 mM, and 20 mM) were perfused in mature chips for 3 days, and the albumin assay was conducted on the chip, as explained earlier.

Statistics

The data are reported as mean ± standard error (SE) values. Statistically significant differences between the experimental groups have been also analyzed using parametric, two-tailed Student's tests, whereas one-way analysis of variance for more than two experimental groups was calculated by Graphpad Prism. The *p, **p, ***p values, which respectively represent 0.05, < 0.01, < 0.001, denote statistically significant outcomes.

Declarations

Acknowledgments: xxx.

Funding: This research study was supported by the National Research Foundation of Korea (NRF) grants (NRF-2020M3H4A1A02084827) and by the Brain Pool Program grant (2017H1D3A1A02053559) funded by the Ministry of Science and ICT.

Author contributions: N.K.S. and D.-W.C. conceived the research concept, analyzed the data and wrote the manuscript. N.K.S. designed the research and performed the experiments. J.Y.K., J.Y.L., H.L., G.G., J.J., and Y.K.M. designed the study and prepared the illustrations and figures.

Competing interests: The authors declare no competing interests.

Data availability: All results related to this research study have been presented within this paper and its supplementary files.

References

1. Daehn, I.S. & Duffield, J.S. The glomerular filtration barrier: a structural target for novel kidney therapies. *Nature Reviews Drug Discovery* **20**, 770-788 (2021).

2. Du, B., Yu, M. & Zheng, J. Transport and interactions of nanoparticles in the kidneys. *Nature Reviews Materials* **3**, 358-374 (2018).

3. Scott, R.P. & Quaggin, S.E. The cell biology of renal filtration. *Journal of cell biology* **209**, 199-210 (2015).

4. Suh, J.H. & Miner, J.H. The glomerular basement membrane as a barrier to albumin. *Nature Reviews Nephrology* **9**, 470-477 (2013).

5. Farquhar, M.G. The primary glomerular filtration barrier—basement membrane or epithelial slits? *Kidney international* **8**, 197-211 (1975).

6. Haraldsson, B., Nyström, J. & Deen, W.M. Properties of the glomerular barrier and mechanisms of proteinuria. *Physiological reviews* (2008).

7. Menon, M.C., Chuang, P.Y. & He, C.J. The glomerular filtration barrier: components and crosstalk. *International journal of nephrology* **2012** (2012).

8. Levin, A. et al. Global kidney health 2017 and beyond: a roadmap for closing gaps in care, research, and policy. *The Lancet* **390**, 1888-1917 (2017).

9. Flegeau, K. et al. Towards an in vitro model of the glomerular barrier unit with an innovative bioassembly method. *Nephrology Dialysis Transplantation* **35**, 240-250 (2020).

10. Musah, S. et al. Mature induced-pluripotent-stem-cell-derived human podocytes reconstitute kidney glomerular-capillary-wall function on a chip. *Nature biomedical engineering* **1**, 1-12 (2017).

11. Petrosyan, A. et al. A glomerulus-on-a-chip to recapitulate the human glomerular filtration barrier. *Nature communications* **10**, 1-17 (2019).

12. Wang, L. et al. A disease model of diabetic nephropathy in a glomerulus-on-a-chip microdevice. *Lab on a Chip* **17**, 1749-1760 (2017).

13. Homan, K.A. et al. Flow-enhanced vascularization and maturation of kidney organoids in vitro. *Nature methods* **16**, 255-262 (2019).

14. Morizane, R. & Bonventre, J.V. Kidney organoids: a translational journey. *Trends in molecular medicine* **23**, 246-263 (2017).

15. Shi, Y., Inoue, H., Wu, J.C. & Yamanaka, S. Induced pluripotent stem cell technology: a decade of progress. *Nature reviews Drug discovery* **16**, 115-130 (2017).

16. Lee, D.W., Choi, N. & Sung, J.H. A microfluidic chip with gravity-induced unidirectional flow for perfusion cell culture. *Biotechnology progress* **35**, e2701 (2019).

17. Wang, Y.I. et al. Self-contained, low-cost Body-on-a-Chip systems for drug development. *Experimental biology and medicine* **242**, 1701-1713 (2017).

18. Gao, G. et al. Construction of a Novel In Vitro Atherosclerotic Model from Geometry-Tunable Artery Equivalents Engineered via In-Bath Coaxial Cell Printing. *Advanced Functional Materials* **31**, 2008878 (2021).

19. Liang, Q. et al. Coaxial Scale-Up Printing of Diameter-Tunable Biohybrid Hydrogel Microtubes with High Strength, Perfusability, and Endothelialization. *Advanced Functional Materials* **30**, 2001485 (2020).

20. Pi, Q. et al. Digitally tunable microfluidic bioprinting of multilayered cannular tissues. *Advanced Materials* **30**, 1706913 (2018).

21. Singh, N.K. et al. Three-dimensional cell-printing of advanced renal tubular tissue analogue. *Biomaterials* **232**, 119734 (2020).

22. Han, W. et al. Directed differential behaviors of multipotent adult stem cells from decellularized tissue/organ extracellular matrix bioinks. *Biomaterials* **224**, 119496 (2019).

23. Kim, B.S., Das, S., Jang, J. & Cho, D.-W. Decellularized extracellular matrix-based bioinks for engineering tissue-and organ-specific microenvironments. *Chemical Reviews* **120**, 10608-10661 (2020).

24. Pati, F. et al. Printing three-dimensional tissue analogues with decellularized extracellular matrix bioink. *Nature communications* **5**, 1-11 (2014).

25. Homan, K.A. et al. Bioprinting of 3D convoluted renal proximal tubules on perfusable chips. *Scientific reports* **6**, 1-13 (2016).

26. Jang, K.-J. et al. Human kidney proximal tubule-on-a-chip for drug transport and nephrotoxicity assessment. *Integrative Biology* **5**, 1119-1129 (2013).

27. Lin, N.Y. et al. Renal reabsorption in 3D vascularized proximal tubule models. *Proceedings of the National Academy of Sciences* **116**, 5399-5404 (2019).

28. Abrahamson, D.R. in Seminars in nephrology, Vol. 32 342-349 (Elsevier, 2012).

29. Abrahamson, D.R., Hudson, B.G., Stroganova, L., Borza, D.-B. & John, P.L.S. Cellular origins of type IV collagen networks in developing glomeruli. *Journal of the American Society of Nephrology* **20**, 1471-1479 (2009).

30. Cosgrove, D., Kalluri, R., Miner, J.-H., Segal, Y. & Borza, D.-B. Choosing a mouse model to study the molecular pathobiology of Alport glomerulonephritis. *Kidney international* **71**, 615-618 (2007).

31. Funk, S.D., Lin, M.-H. & Miner, J.H. Alport syndrome and Pierson syndrome: Diseases of the glomerular basement membrane. *Matrix Biology* **71**, 250-261 (2018).

32. Delézay, O. et al. Glomerular filtration drug injury: In vitro evaluation of functional and morphological podocyte perturbations. *Experimental cell research* **361**, 300-307 (2017).

Figures

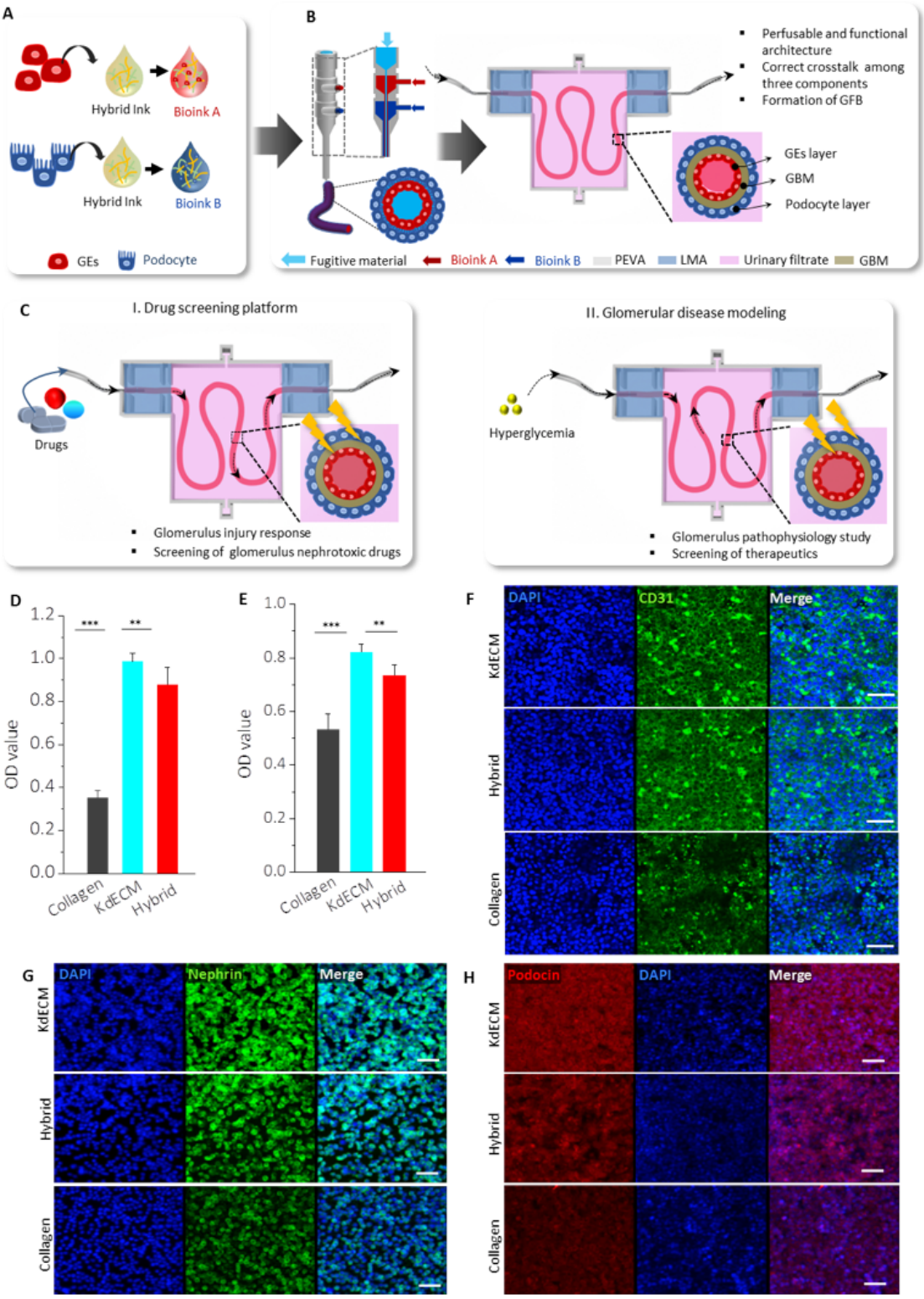

Figure 1

Illustration of glomerular research strategy and functional assessment of glomerular cells with customized bioink. (A) Preparation of kidney tissue-specific hybrid bioink to encourage the functional behaviors of glomerular endothelial (GEs) and podocytes. **(B)** Three-dimensional (3D) coaxial cell printing of a functional bilayer glomerular microvessel-on-a-chip (bGOAC). **(C) (i)** Modeling of glomerular injury and proteinuria *in vitro*, and **(ii)** establishment of diabetic nephropathy in bGOAC. **(D)** GEs and **(E)**

podocytes showed significantly higher cell viability in pure 3% (w/v) kidney decellularized extracellular matrix (KdECM) and hybrid bioink (3K1A), compared with 3% (w/v) collagen type I over a culture period of 7 days (**p < 0.01, ***p < 0.001). **(F)** The hybrid bioink (3K1A) resulted in higher expressions of the vascular endothelial cells marker CD31 and **(G, H)** podocyte specific markers nephrin and podocin than 3% (w/v) collagen type I (scale bars, 50 μm).

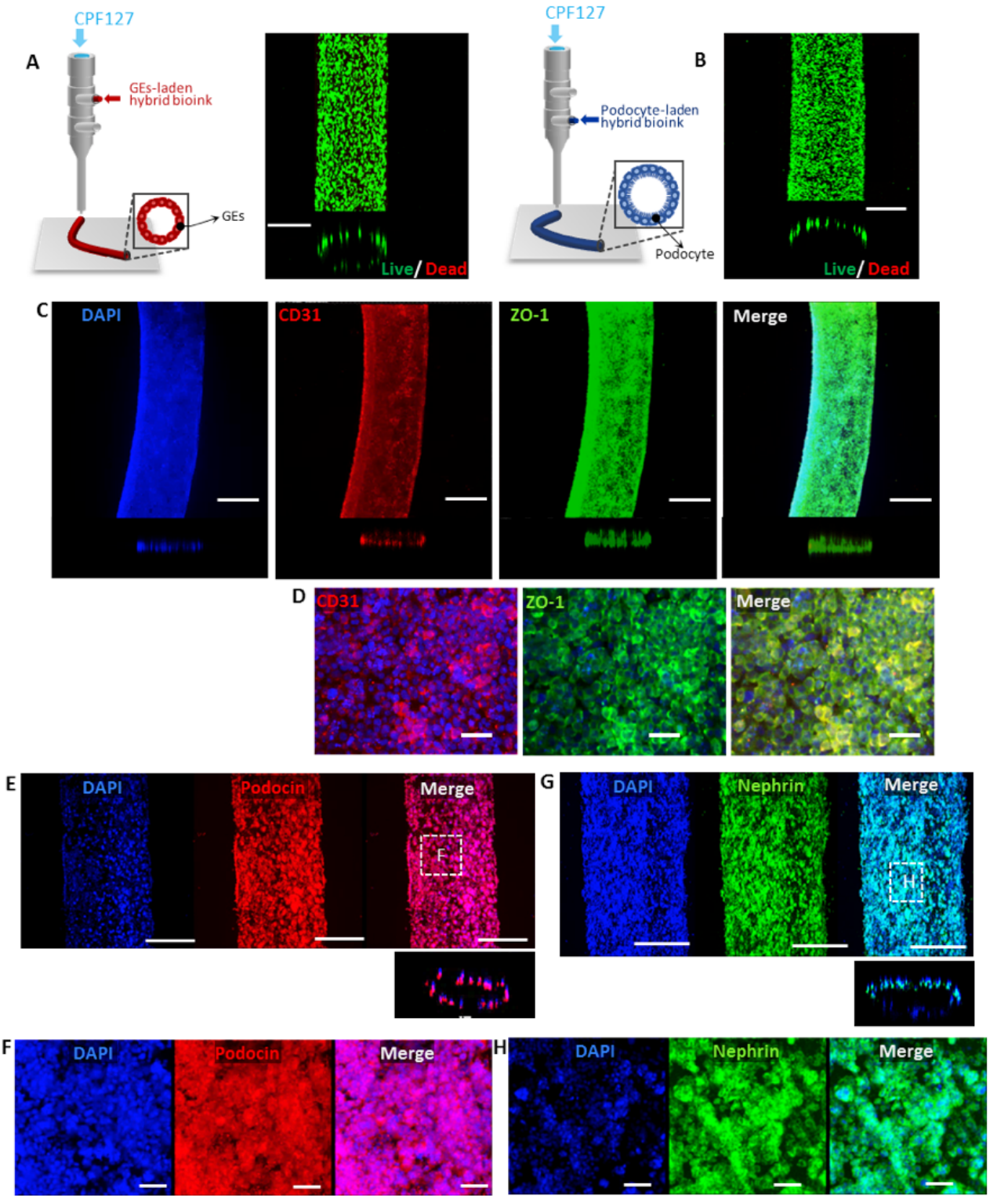

Figure 2

Direct coaxial cell printing of perfusable GE and podocyte tubes. (A) GEs, **(B)** podocyte-laden 3K1A hybrid bioink facilitates the printing and cellular maturation of GE and podocyte tubes, respectively (scale bars, 500 μm). **(C, D)** Immunofluorescence stainings of the vascular endothelial cell-specific marker CD31 and tight junction marker ZO-1 confirming the confluence monolayer of endothelium in the mature GE tube after 7 days of culture (scale bars, 500 μm, 50 μm). Podocyte-specific stainings of markers podocin **(E, F)** and nephrin **(G, H)** validate the confluence monolayer of epithelium in a mature podocyte tube on day 7 (scale bars, 500 μm, 50 μm).

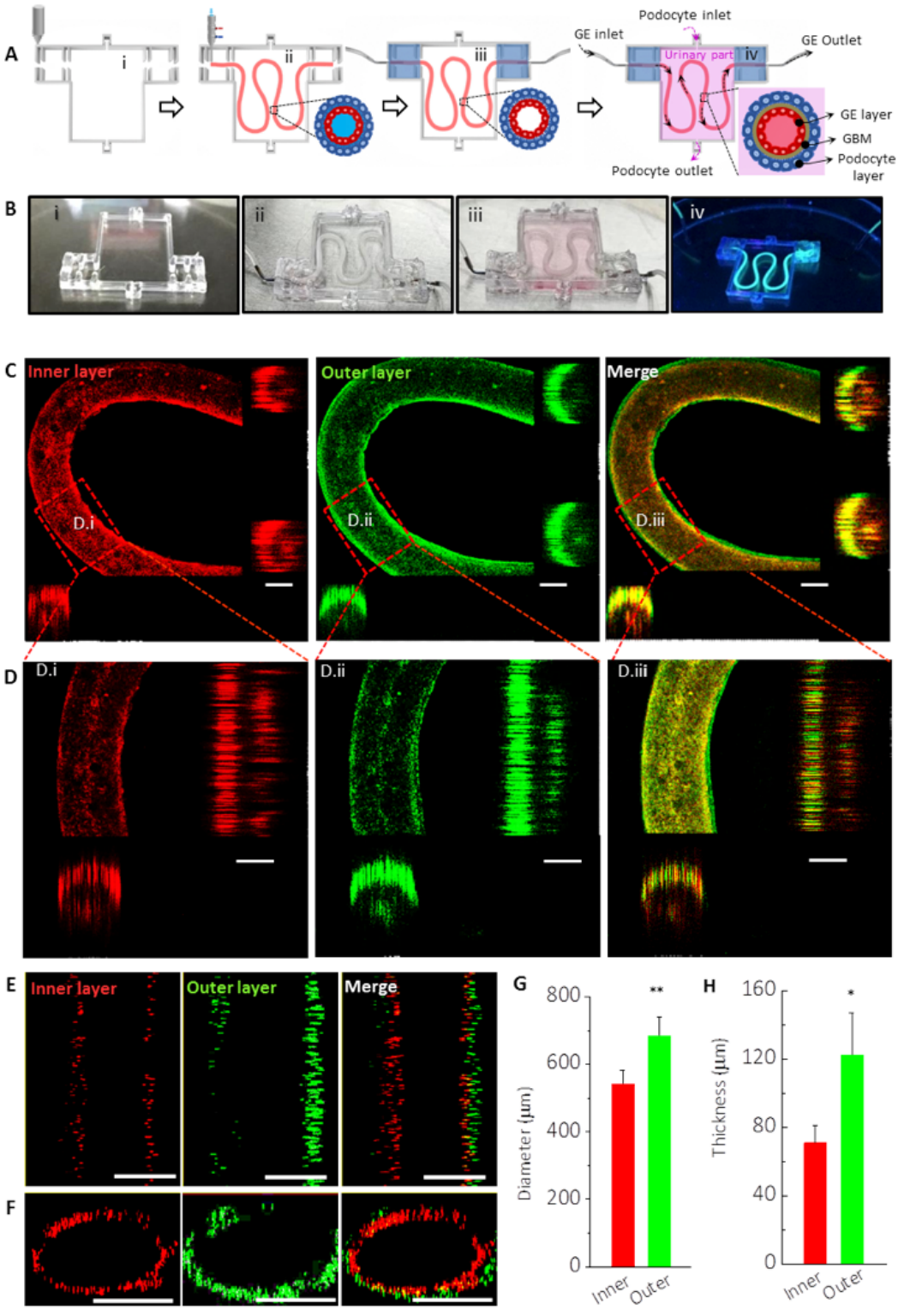

Figure 3

Construction of bGOAC. (A) Schematic representation of bGOAC fabrication steps, including: **(B) (i)** 3D printed poly(ethylene/vinyl acetate) (PEVA)-based chip body, **(B) (ii)** coaxial cell-printed bilayer glomerular microvessel using GEs and podocyte-laden hybrid bioinks (3K1A), and subsequent inlet/outlet fixation through the casting of low melting agarose (LMA), and **(B) (iii, iv)** perfused bGOAC containing bilayer glomerular microvessel. **(C, D)** Confocal images displaying the successful construction of bilayer glomerular microvessels (scale bars, 500 μm). **(E, F)** Representative cross-sectional confocal image views of inner (red) and outer (green) walls of the bilayer glomerular microvessel (scale bars, 500 μm). **(G, H)** Average diameter and thickness of inner and outer layers of bilayer glomerular microvessel (*$p < 0.05$, **$p < 0.01$).

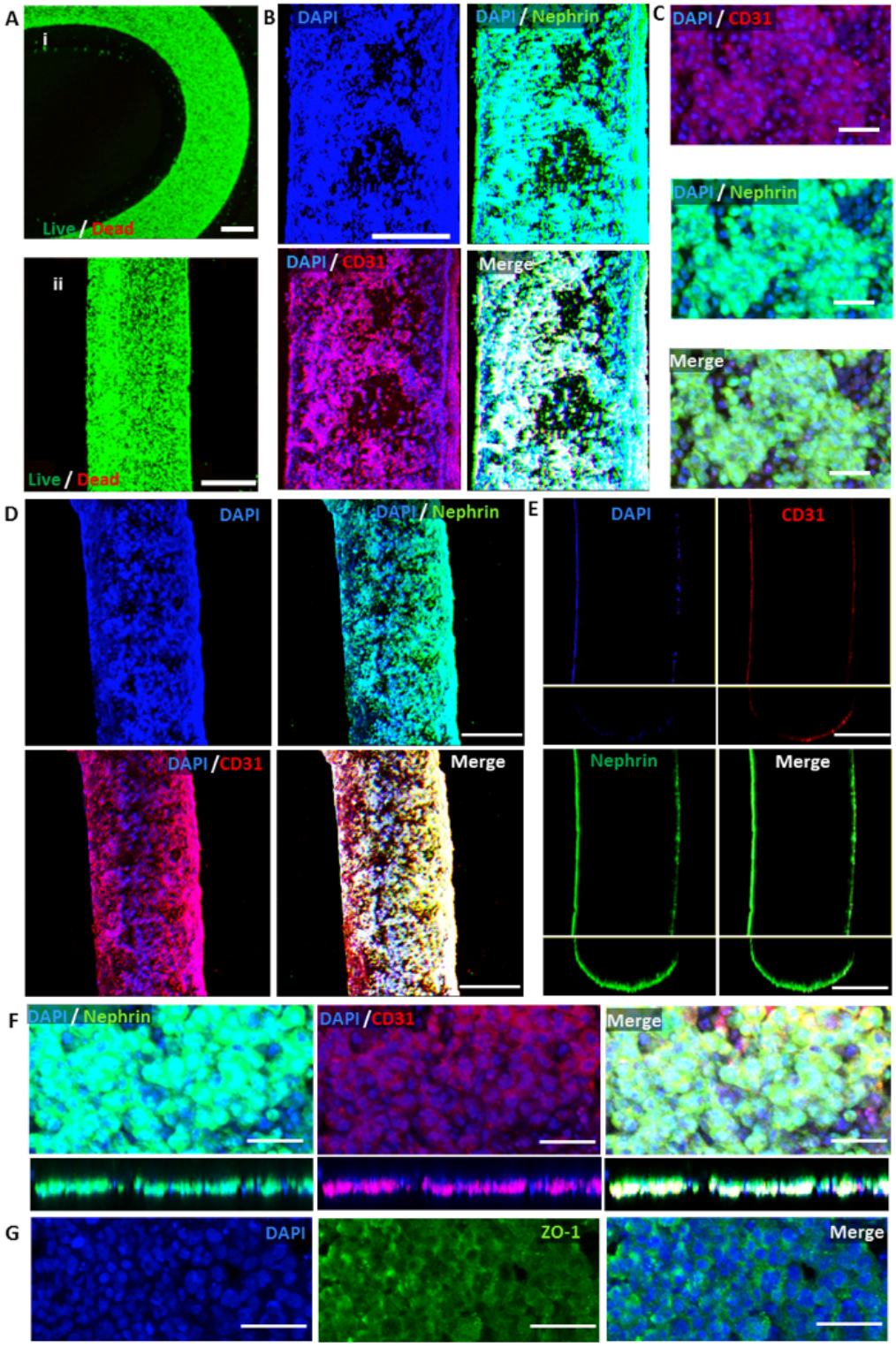

Figure 4

Maturation of the glomerular equivalent bGOAC. **(A) (i, ii)** Live–dead images of glomerular cells (podocyte, GEs) within layers of the coaxial, cell-printed bGOAC on day 1 and 7. Confocal images of the immunostained bGOAC after 3 days **(B, C)** and 7 days **(D-G)** showing the expressions of vascular endothelial specific marker CD31, podocyte specific marker nephrin, and tight junction zonula occludens (ZO-1) marker (scale bars, 500 μm, 50 μm).

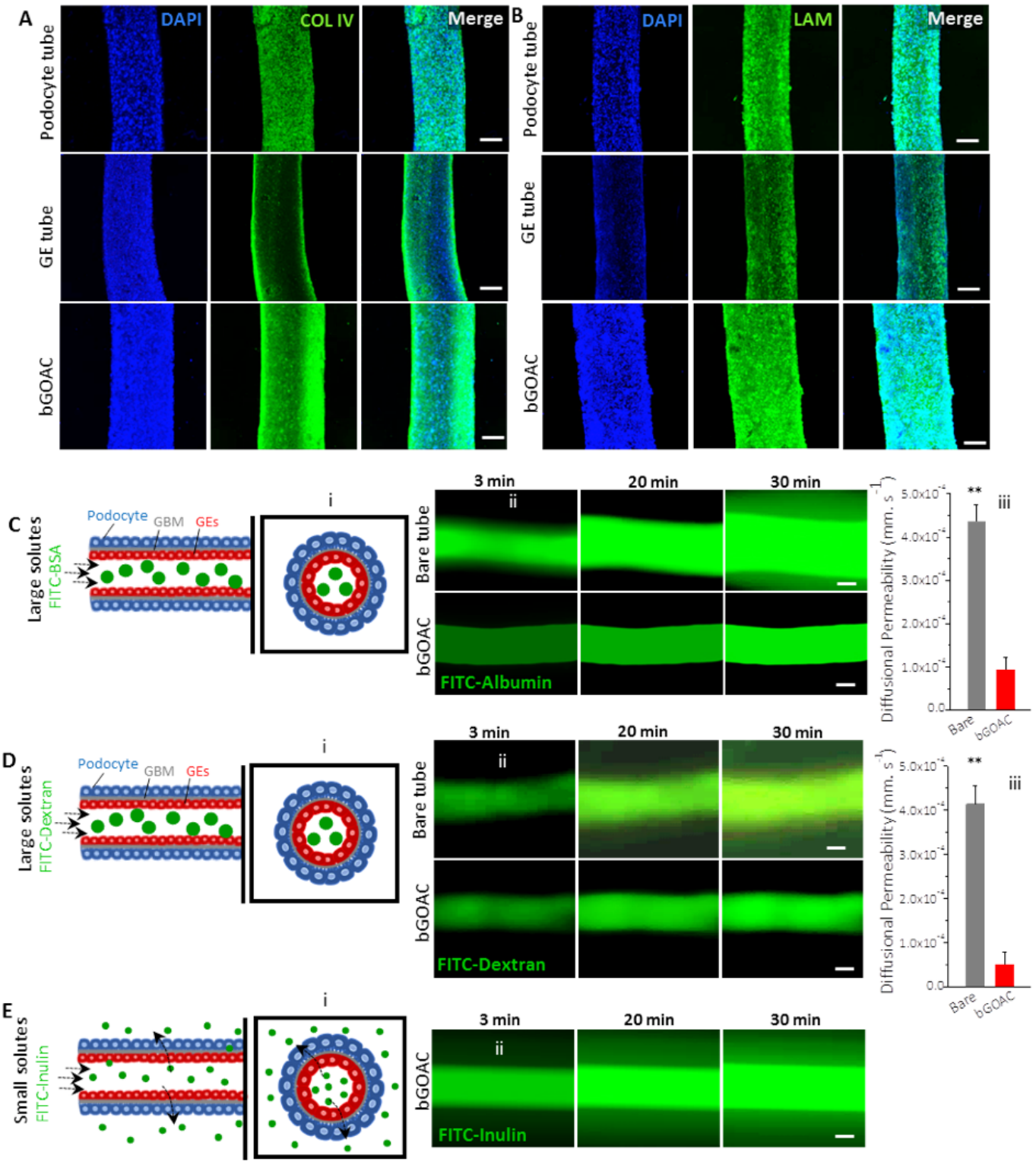

Figure 5

Formation of glomerular basement membrane (GBM) and permselectivity of functional glomerular model. Confocal images displaying the production and distribution of GBM proteins **(A)** COL IV and **(B)** LAM in perfusable podocyte tube, GE tube and bGOAC on day 7 (scale bars, 300 μm). Fluorescein isothiocyanate (FITC)–albumin and FITC–dextran perfused to the bGOAC and fluorescent images **(C)** FITC–albumin, **(D)** FITC-dextran show reduced diffusion of large solutes from the bGOAC and

significantly decreased diffusion permeability compared with those in the bare tube. **(E)** Perfusion of inulin–FITC reveals significant diffusion of small solutes from the bilayer glomerular microvessel to the urinary part (scale bars, 500 μm; **p < 0.01).

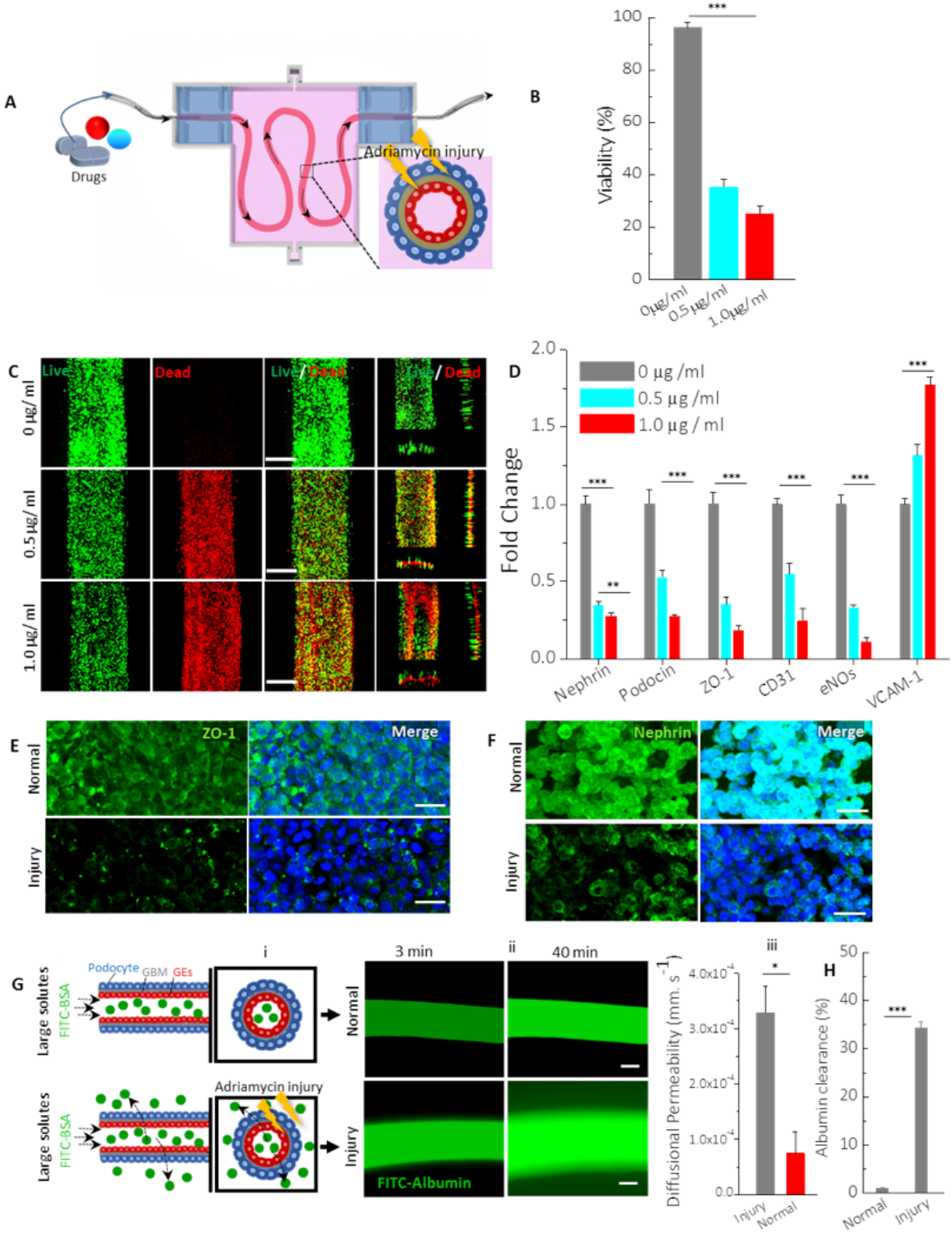

Figure 6

Recapitulation of drug-induced glomerular injury by the bGOAC. (A) Schematic representation of Adriamycin exposure to mature chip for 3 days and glomerular injury. **(B, C)** Cell viability of glomerular cells within the bGOAC continuously perfused with different doses of Adriamycin (***p < 0.001, scale bars, 500 μm). **(D)** Increased VCAM-1 gene expression marker and decreased expressions of vascular endothelial cells specific marker CD31, tight junction marker ZO-1, and podocytes specific markers (nephrin, podocin) after different concentrations of Adriamycin are exposed to bGOAC (*p < 0.05, **p < 0.01, ***p < 0.001). **(E, F)** Confocal microscopy images of the immunostained bGOAC after 1.0 μg mL^{-1} Adriamycin exposure for 3 days (scale bars, 30 μm). **(G) (i, ii)** Fluorescence images indicating leakage of albumin after 3 min and 40 min, and drastically enhanced albumin diffusion permeability in bGOAC after Adriamycin treatment (1.0 μg mL^{-1}) (scale bars, 500 μm). **(H)** Quantification of albumin clearance in normal and damaged bGOACs (*p < 0.05).

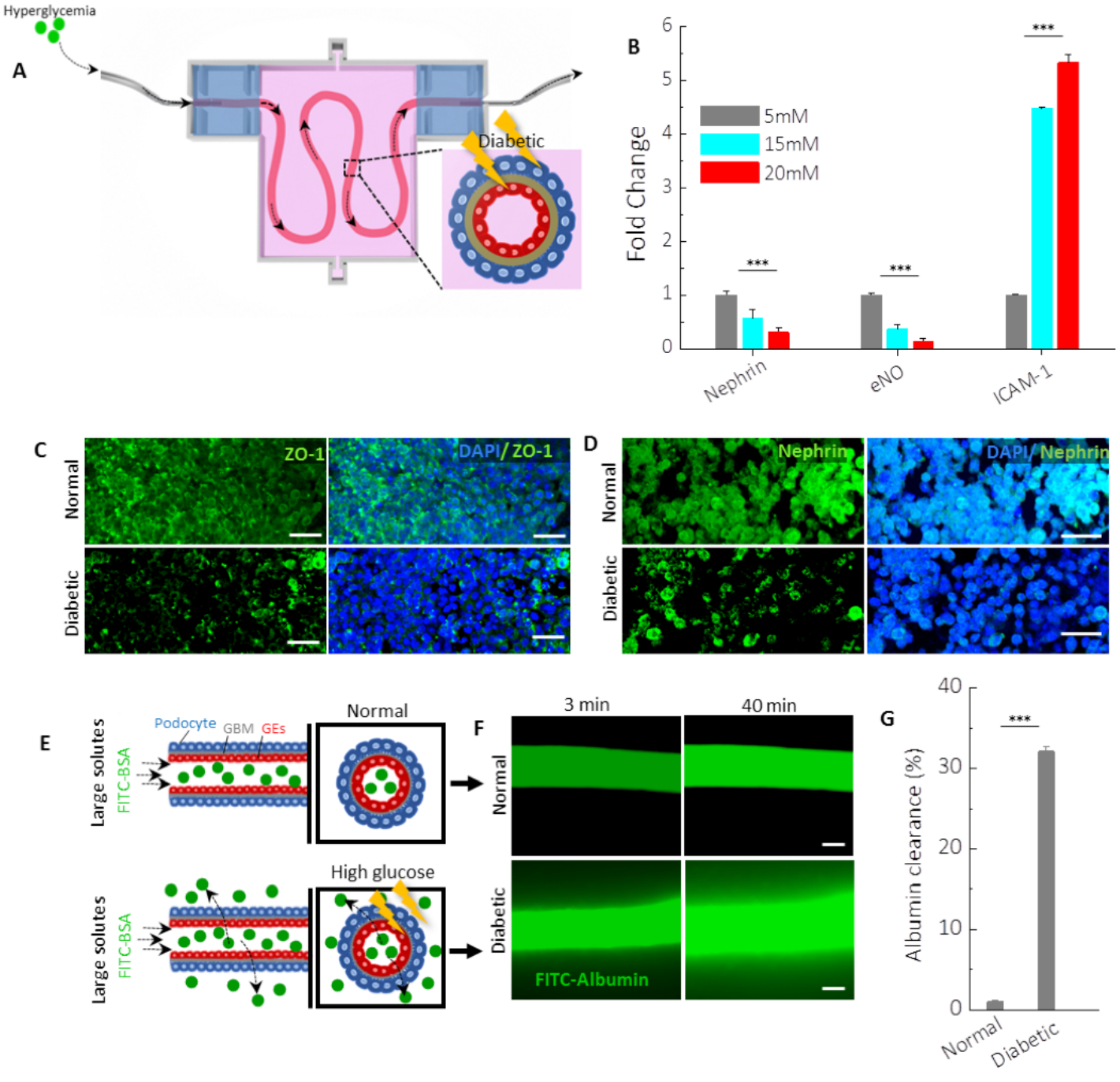

Figure 7

Establishing diabetic nephropathy in bGOAC. **(A)** Perfusion of different concentrations of glucose in the mature bGOAC for 3 days to induce diabetic nephropathy. **(B)** Upregulation of the gene expression of ICAM-1 marker and downregulation of expressions of vascular endothelial cell-specific markers CD31, eNOs, and podocyte-specific marker nephrin after different concentrations of glucose are exposed to bGOAC (***p < 0.001). **(C, D)** Confocal images of the immunostained bGOAC after glucose exposure (concentration: 20 mM) for 3 days (scale bars, 50 μm). **(E, F)** Fluorescence images demonstrating leakage of albumin after 3 min and 40 min, and drastically enhancement of albumin diffusion

permeability in bGOAC after treatment with high concentrations of glucose (scale bars, 500 μm). **(G)** Quantification of albumin clearance in normal bGOAC and diabetic bGOAC (***p < 0.001).

Supplementary Files

This is a list of supplementary files associated with this preprint. Click to download.

- Supplementaryfile.docx
- SupplementaryVideo1.Printing.mp4
- SupplementaryVideo2.Perfusion.mp4